Etude # 236
IGM85-205-236

Recrystallization model for controlling the mechanical properties obtained with batch annealed cold rolled low carbon aluminum killed steel sheets

R. Thibau, J. Masounave,
Industrial Materials Research Institute
National Research Council Canada
75, blvd. de Mortagne
Boucherville, Québec, Canada J4B 6Y4

and

L. Piperni,
Sidbec Dosco Contrecoeur
C.P. 1000, Contrecoeur, Québec J0L 1C0

CNRC 24864

ABSTRACT

The mechanical performance of a cold rolled batch annealed aluminum killed steel sheet depends greatly on the composition of the steel and on the thermomechanical parameters of the process. The role of carbon, aluminum and nitrogen contents as well as the coiling temperature, the cold reduction percentage and the thermal characteristics of the batch annealing treatment are reviewed in light of new experimental results. A proposed model explaining the various effects of the processing parameters gives a consistent interpretation of the results, and constitutes a valuable tool for predicting the quality of a sheet.

1.- INTRODUCTION

The mechanical properties of cold rolled aluminum killed steel sheets after annealing, are controled by their chemical composition and the thermomechanical variables. It is important for the steel industry to be able to predict with consistency the quality of their product. Unexpected high yield strengths can result in considerable economical losses. The effects of fine precipitates on the recrystallization mechanisms in steel sheets are essential in the formation of the recrystallized texture and thus the formability as defined by the plastic anisotropy, r [1-4]. It is well known that AlN precipitates, formed during recovery on the sub-grain boundaries, can interfere with recovery and sub-boundary mobility and therefore modify the nucleation process [3, 5, 6]. Some authors [7-12] have shown how (111) subgrains recover faster than (100) subgrains, which subsequently results in a selection of the recrystallization nuclei by the Zener drag effect due to AlN particles. As recrystallization and precipitation take place simultaneously, it is important to be able to understand the effect of AlN precipitation kinetics on the growth kinetics of the various grains' orientations. Several authors [13-15] have observed a recrystallization interruption, due to AlN precipitation, which results in a delay of the end of primary recrystallization. A complementary explanation of the circumstances which lead to this anomaly is given in this paper.

The purpose of the present paper is to suggest a simple model which can be used to predict, semi-quantitatively, the effects of the main

variables, such as aluminum, carbon and nitrogen contents, the cold reduction percentage and the furnace holding time.

2.- EXPERIMENTAL PROCEDURE

The principle of the experimental program was to simulate, for various steel compositions, the cold rolling and annealing industrial processes: hot rolled sheet samples, from continuous cast slabs, were cold rolled on an experimental rolling mill to 40 and 70 % reductions. The tensile samples, machined according to ASTM E517 Standard, were subsequently annealed under a purified argon atmosphere. The experimental furnace was programmed to simulate the time temperature cycles recorded at the cold spot in an industrial single stack batch annealing furnace. The average heating rates, between 200 and 500°C, varied from 28 to 55°C/hr, the holding times varied between 10 and 25 hours and the maximum temperatures reached varied between 610 and 737°C (see table 1).

The tensile tests were performed on samples oriented along the longitudinal (L), the transversal (T), and the 45° diagonal directions relative to the rolling direction. The deformation rate was kept constant at $1.1 \times 10^{-3} s^{-1}$. The mechanical parameters measured, the yield strength, the plastic anisotropy ratio and the strain hardening rate, respectively Sy, r and n, were averaged following the standard formula: $Sy = 1/4(S_L + 2S_D + S_T)$. A data acquisition system was used with the tensile test which allowed the calculation of the incremental

plastic anisotropy [17], $r=\partial\varepsilon_w/\partial\varepsilon_t$ (w and t are for width and thickness dimensions), which is a more accurate measurment of plastic anisotropy, $R=\varepsilon_w/\varepsilon_t$, since Lüders bands are present [17]. The values reported were all measured at 15 % deformation. The strain hardening rate, n, is calculated, following Hollomon's equation $\sigma=K\varepsilon^n$, between 10 % and 22 % deformations.

Four steel compositions, with two aluminum content levels (.04% and .06%) were investigated, see table 2. Each hot rolled sheet sample was obtained from hot rolled bands coiled at both 560°C and 700°C. The solution temperature of the slabs prior to hot rolling was 1260°C and the last finishing hot rolling pass temperature was kept above 840°C. Steels identified with odd numbers had all their nitrogen precipitated prior to cold rolling.

As can be noted the compositions and thermo-mechanical parameters used in this projects are common industrial practices.

3.- RESULTS

All mechanical results are plotted versus a thermal parameter Pq and, for the practical reference, versus the maximum temperature, Tm, reached by the cold spot during annealing. The yield strength, Sy, is shown in Fig. 1, the plastic anisotropy, r, in Fig. 2 and the strain hardening rate, n, in Fig. 3.

The thermal parameter Pq, time and temperature dependant, is defined by similarity between recrystallization and Fe self-diffusion[18].

$$Pq = -10^4 (R/Q)\ \mathrm{Log}_e \left(\int_{t_1}^{t_2} \exp(-Q/RT)\,dt \right)$$

where t=time (hours), R=1.989 (cal.mole $^{-1}$) T=temperature (K) and Q=60 (kcal.mole $^{-1}$). Several authors [18] have calculated the activation energy of recrystallization and grain growth and, as expected, have found large variations as recrystallization can be slowed down or even interrupted completely by particles. An average value of 60 kcal mole^{-1} was chosen which is also not far from the activation energy of Al diffusion in ferrite [19]. The times t_1 and t_2 are defined by the portion of the annealing cycle where $T > 823K$ (550°C). The Pq value varies between 10.7 and 9.1K^{-1} which is representative of the annealing treatment for commercial and deep drawing qualities. If either the holding time or the temperature increase, i.e. the energy input per unit mass of annealed steel increases, the value of Pq decreases.

4.- OBSERVATIONS AND INTERPRETATIONS

The heating rate variation, as shown in table 2, does not result in substantial effects of the mechanical properties. We can assume that the heating rate variation range is not large enough to affect sufficiently the balance of the recovery and AlN precipitation kinetics. Therefore, the heating rate is taken into account only through the calculation of the value of Pq.

a) Yield strength

Fig. 1 shows the effect of the annealing cycle (Pq or Tm) on the yield strength; it appears that, when Pq is high, an abnormally high yield strength is obtained for lower Al contents (.04 %) steels when cold rolled at lower reduction levels (40 %). This effect increases when the nitrogen content is higher (70 ppm) and when the coiling temperature is low (560°C) (see fig. 1a and 1c). When the aluminum content is higher (.06%) or when the cold reduction is higher (70 %) no such abnormally high yield strength appears at high Pq values. As shown in the discussion, these anomalies can be related to recrystallization delays due to AlN precipitates.

A carbon increase generally results in an increase in the yield strength except in the case of lower coiling temperature with lower cold reduction (Fig. 1a). At a higher coiling temperature, 700°C, a .03 % increase in carbon content results in a 50 MPa increase in the yield strength. It is known that an increase in the carbide population or size, due to either a carbon content increase or a higher coiling temperature [20], will accelerate the nucleation rate and therefore raise the yield strength level [21]. Humphreys [21] has also shown that nucleation at large particles depends on both the amount of cold reduction and the size of the particles: the smaller the particle size, the higher the critical reduction level needed for the particles to become nuclei. As shown by Fig. 1a, the finer carbides obtained when the coiling temperature is 560°C does not significantly affect the nucleation rate when the cold reduction is 40 %

b) Plastic anisotropy ratio

The plastic anisotropy ratio, r, as shown in Fig. 2, is consistently higher with steel containing lower aluminum levels (.04 %) and also, as expected, for higher cold rolling reduction (70 %) or lower coiling temperatures (560°C). An increase of .03 % in carbon content (steel 01/02 vs steel 03/04) has a clear weakening effect on r (Fig. 2b) when the coiling temperature is 560°C but not with a cold reduction level of 40 % (Fig. 2a). As with the yield strength, the effect of carbon can be related to the nucleation rate: carbide linked nuclei produce more randomly oriented grains and therefore deteriorate the resulting texture.

The weakening of the recrystallization texture obtained when the Al content is .06 %, as explained in more detail in the discussion, is the result of incomplete solution of AlN particles in the slab when it is soaked at 1260°C [21]. The actual volume fraction left for the nuclei selection during recovery and recrystallization is reduced. As the Al content increases, the final texture after annealing is substantially affected. Fig. 1a and 1b show that a .02 % increase in Al can result in a drop of approximately 20% of the r value.

c) Strain hardening rate

The work hardening rate, n, is related to the way arrays of dislocations are stored by the ferrite matrix [23]. The variables usually cited

[2] as influencing n, are the grain size, the precipitates (AlN) and the alloying elements in solution in the ferrite (Cu, Si, Mo, Mn, Ni).

Blickwede [2] has shown empirically that n follows a simple expression:

$$n=5/(10+D^{-1/2})$$

where D is the grain size.

Fig. 3 shows that n increases consistently with grain growth (with diminishing Pq values). Also, increasing the cold reduction decreases the n value. The lowest yield values, obtained with steel 03/04, gives the highest n values.

Ashby [22] has shown that the density of geometrically necessary dislocations, ρ , is inversely proportionnal to the mean free path, λ of these dislocations:

$$\rho=k/\lambda \text{ and } \lambda=r/f$$

where k is a constant, r is the particle radius and f their volume fraction.

In the present case, the steels for which n values would be most influenced by AlN precipitates (r=100A) are steel 01/02 (λ=17μm) and the least affected is steel 03/04 (λ=30μm). This can explain why the curves in Fig. 3 of steel 01/02 are consistently higher than expected from the yield strength curves (Fig. 1). Ichiyama et al [24] have also reached a similar interpretation.

Among the various elements in solid solution, manganese is the only one, whose variation of .1 % (corrected for sulfur content), should be taken into account. Unfortunately, the literature [2,25] is contradictory on the effect of Mn. The high n values obtained here with 03/04 steel in Fig. 1a leads one to think that, as Hu [25] reported, a .1 % increase in Mn content results in approximately a .01 increase in n. Apparently the prediction of n values should be primarily based on the grain size, secondary factors such as AlN morphology and Mn content should also be considered.

5.- DISCUSSION

The theory of Hillert [26], used by Meyzaud et al [27] and others [5,6], on grain growth applied to subgrains having a given size distribution characterized by the medium size D_m and the maximum size, D_M, or the size factor t:

$$t=D_M/D_m \qquad \text{eq. 1}$$

gives the following expression for the driving force per unit area of sub-boundary:

$$F_H=2\gamma(1/D_m-1/D) \qquad \text{eq. 2}$$

where D is the size of the subgrain considered and γ is the sub-boundary surface energy. F_H is at its maximum value for the largest subgrains which gives us the following expression:

$$F_H=(2\gamma/D_m)\ (1-1/t) \qquad \text{eq. 3}$$

When particles are interacting with subgrain boundaries they create a

drag force, F_Z, which counteracts the driving force [6]:

$$F_Z=\pi\gamma Ps\ d/2 \qquad \text{eq. 4}$$

where d is the average particle diameter and Ps is the number of particles interacting with the sub-boundary [27].

It has been shown that AlN precipitation takes places along grain boundaries and sub-boundaries [15]: in that case, for a typical equiaxed subgrain shape (V/S=D/3.35, where V, S and D are the volume, the boundary area and the diameter of the grain), the Ps value is given by the following expression [27]:

$$Ps=(1.8/\pi d^3)\ f\ D_m \qquad \text{eq. 5}$$

where f is the AlN precipitated volume fraction.

From equations 4 and 5 F_Z is obtained:

$$F_Z=.9\gamma f(D_m/d^2) \qquad \text{eq. 6}$$

The equilibrium condition of the sub-boundary most susceptible to migrate ($D=D_M$) is:

$$F_Z=F_H \qquad \text{eq. 7}$$

Equation 7 determines the critical size, dc, to which the AlN particles have to grow in order to release the sub-boundary [27].

$$d_c=(.45f/(1-1/t))^{1/2}.\ D_m \qquad \text{eq. 8}$$

A- Effect of the size factor t

Well known experimental results [3, 7, 8] have shown that AlN particles can delay the recovery process particularly for the (100) cells and affect to a lesser degree the (111) cells. It was also observed that most of the first grains to recrystallize had a (111) orientation [28]. It can therefore be supposed [7, 29] that the rate of nucleation is higher in (111) grains, and as a consequence the size factor is larger for the subgrain having the (111) orientation as compared to (100) subgrains. Fig. 4 shows d_c curves obtained for an average subgrain size of 1.0μm and for t values varying from 1.5 to 10 (eq. 8). High t values, such as t=10, are representative of the size factor existing between a recrystallized grain growing inside the unrecrystallized matrix. It can be noticed that, for a given precipitated volume fraction, as the size factor increases, the critical AlN size decreases and tends rapidly to a minimum value (eq. 8).

B- Effect of AlN size

The actual AlN size, d_p, during precipitation on sub-boundaries depends on the number of precipitates per unit volume, P, and the effective precipitated volume fraction f (i.e. the precipitates which are actually formed on the sub-boundaries).

$$f=\pi d_p{}^3 P/6 \qquad \text{eq. 9}$$

This gives the following particle size:

$$d_p = 1.24\ (f/P)^{1/3} \qquad \text{eq. 10}$$

The precipitation of AlN is regulated by the slow diffusion of aluminum to sub-boundaries where nitrogen has segregated [19]. Because of their strong influence on recovery, it is reasonable to consider that the number of precipitates reaches its final value, P_o, soon after precipitation starts as in a quasi-saturated site nucleation.

Fig. 4 represents the d_p curves obtained with a saturated precipitation site nucleation and with P_o values of 5×10^{20} and $10^{21} m^{-3}$ which are in agreement with experimental values obtained by Furubayashi et al [30].

C- Nuclei selection mechanisms

Fig. 4 represents for example the case where D_m, the average subgrain size, is 1.0μm and $P_o = 10^{21} m^{-3}$: for a precipitated volume fraction of 10^{-5} (approximately 2ppm of precipitated nitrogen) the particle size is approximately 27Å (see Fig.4); let t_o be the value of t for the d_c curve passing through this point. Thus, subgrains having a size factor $t \leq t_o$ are pinned while subgrains which have developed a size factor $t > t_o$ continue to recrystallize. Depending on the actual amount of nitrogen which is precipitating, P, the value of t_o will increase with f and the selection operated will eliminate the slow

recovery subgrain orientations. As f increases, a complete interruption of recrystallization is possible. In the example shown in Fig. 4, recrystallization is interrupted for $f = 10^{-5}$. As precipitation ends, particle growth through coalescence takes place. The kinetics of coalescence are given by power laws of time with exponents equal 1/3, 1/4 or 1/5 in the cases of bulk, grain boundary or pipe diffusion [31, 32], while the exponent is equal to 1/2 during precipitation [33]. The diameter growth rate during coalescence is lower than during precipitation. Consequently, when primary recrystallization is regulated by AlN coalescence, a stronger size factor selection is promoted which should again favor the (111) orientations. From this, it is possible to predict that a larger effective precipitated volume fraction results in a stronger (111) texture and a larger plastic anisotropy ratio. Nevertheless, from a practical point of view, it does not seem to be advantageous to stop completely recrystallization as this would lead to long and costly annealing treatments together with too large a grain size.

D- Factors that influence the effective precipitated volume fraction

In continuous cast slabs, the aluminum nitrides have to be put back into solution before hot rolling. This is obtained by reheating at a high temperature (1260°C). In austenite, the solubility product, K, was found to be given by the following expression [22]:

$$\log K = \log([Al].[N]) = (-6770/T) + 1.033 \qquad \text{eq. 11}$$

Only steel 01/02 has a K value (5.1×10^{-4}) larger than the equilibrium value at 1260°C (4.6×10^{-4}). Leslie et al [22] have shown that total solution of AlN is actually difficult to obtain for any steel composition with a K value larger than 2×10^{-4}. This is the case for all the samples presently tested. It has been shown also [34] that up to 40% of the nitrogen in solution can precipitate in deformed austenite if the temperature at the final hot rolling pass is 840°C. We therefore have to consider that various amounts of AlN precipitates are already present in the hot rolled band. Since the Al contents of commercial steel composition are always much larger than the stoechiometric level defined by the N content (Al wt % ≈ 2N wt %), any increase in Al content directly reduces the amount of N in solution, whereas if N is increased, the amount of N in solution is slightly increased. Therefore it can be assumed that the amount of nitrogen in solution is increased either by reducing the Al content or increasing the N content [29]. The present results, Fig.1a ($Pq=10.7\ K^{-1}$) indicate that, in agreement with this assumption, higher aluminum content steels (01/02 and 03/04) recrystallize faster than lower aluminum content steels (05/06 and 07/08) which are prone to longer recrystallization delays. The present results indicate also that the plastic anisotropy ratio is improved by lowering the aluminum content and, secondarily, by increasing the nitrogen content (Fig. 2a). The optimized Al and N content values depend on the actual temperature reached during the solution treatment, the temperature of the last finishing hot rolling pass and probably also on other elements present in the steel composition. Ichiyama [29] showed that, at the coiling temperature, any

effect of carbon on AlN precipitation saturates for a carbon content larger than .01 %, therefore it should not have any effect in this case.

E- Effect of cold rolling reduction

Among the principal well known consequences of increasing cold reduction percentages, the decrease in the dislocation cell size [8, 35] and the increase of the (111) orientation density [36] in the cold rolled sheet are considered here. Equation 8 shows that the critical AlN size, d_c, decreases when the value of the subgrain size decreases. The value of the AlN size, d_p (as given by equation 10) is a function of the number of precipitates per unit volume, P. The effect of an increased total area of subgrain boundary per unit volume, S_B, on P, can be approximated by considering that they are proportional:

$$P=kS_B \qquad \text{eq. 12}$$

where k is a constant, P and S_B are respectively the number of precipitates and the total subgrain boundary area, per unit volume. Since S_B is inversely proportional to the subgrain size, D_m (as obtained in a simple cube model), the following expression is obtained:

$$d_p=k.f^{1/3}.D_m^{1/3} \qquad \text{eq. 13}$$

where k is a constant related to the geometry of the subgrains and f is the precipitated volume fraction.

Comparing the values of d_p and d_c, given by equation 8 and 13,

shows that d_c decreases more than d_p when D_m decreases. Therefore any interaction between AlN particles and the subgrain growth tends to decrease when the cold reduction percentage is increased. The resulting improvement in the plastic anisotropy, r, when cold reduction is increased, would therefore be mainly due to increased (111) orientation density in the cold rolled texture. However, .04 % Al steels show a larger plastic anisotropy than .06 % Al steels when the cold reduction is 70 % (Fig. 2b). This indicates that AlN particles are still interacting with recovery and nuclei formation when cold reduction is 70 %. It can also be noted that the difference in r values, between .04 % Al and .06 % Al steels, decreases with increasing cold reduction (Fig. 2a and 2b). This supports the idea that AlN interaction with subgrain growth decreases with increasing cold reductions.

6.- SUMMARY

To summarize, a recrystallization model, using the theory of Hillert on grain growth, some ideas by Meyzaud and Parnière on AlN pinning and the present hypothesis of a variable size factor according to the orientation of the subgrain or grain, all summarized on Fig. 4, can explain the experimental results obtained. In order to be fully quantitative, this model needs additional experimental results in the area of AlN precipitation and subgrain structure. Nevertheless, it is possible, from what has been described here, to predict the effects of the thermo-mechanical treatment and the composition of the steel with a restriction on nitrogen, with lower Al contents (.04%), which cannot be quantified from these results.

7.- CONCLUSIONS

1. The model presented here outlines the major effects of the metallurgical parameters controling the recrystallization of aluminum killed steel sheet.

2. Low cold reduction levels (40 %) with .04 % Al content steel can produce recrystallization delays and therefore higher than expected yield strengths.

3. Improving the plastic anisotropy ratio, r, by lowering the aluminum and carbon contents and/or increasing the nitrogen in solution is more effective and more economical than by increasing the cold reduction or the holding time of the batch annealing furnace.

4. The procedure whereby both r and n are improved is by lowering the carbon content and/or increasing furnace holding time.

5. The heating rate variation used does not have any major effect on the mechanical properties. The thermal parameter, Pq, proposed can be used as the parameter relating time and temperature, for the prediction of the mechanical properties.

Acknowledgement

The authors whish to thank R. Decelles (Sidbec Dosco) and Dr. H. LeHuy (IMRI) for helpfull discussions, D. Simard (IMRI) for his technical assistance and Dr. A. Crawley (CANMET) for his contribution in the cold rolling.

REFERENCES

1. W.B. Hutchinson, Int. Met. Rev., 1984, Vol. 29, n° 1.
2. D.J. Blickwede, Trans. ASM, 61, 1968, 651-79.
3. W.B. Hutchinson, Met. Sci, 1974, 8, 185-96.
4. S. Mishra and C. Därman, Int. Met. Rev. 1982, vol. 27, n° 6, pp 307-20.
5. R. Sandström, Acta Met, vol. 25, pp 905-11, 1977.
6. E. Nes, Acta Met, 24, 391-8, 1976.
7. C.J.E. Smith and J.L. Dillamore, Met. Sci., n° 4, 1970.
8. J.L. Lebrun, G. Maeder, F. Moliexe, P. Parnière, Commission des Communautés Européennes, Report n° EUR 6652 FR, 1980.
9. J.T. Michalak and R.D. Schoone, Trans. A.I.M.E., vol. 242, June 1968, 1149.
10. H. Abe, T. Suzuki, Trans. ISIJ, 1971, 11, 3, 201-10.
11. A.R. Jones and N. Hansen, 1st RISØ Int. Conf., 1980, 13-25.
12. H. Hu and S.R. Goodman, Met. Trans., vol. 1, Nov. 1970, 3057.
13. Y. Meyzaud, P. Parnière and B.J. Thomas, mém. Sci. Rev. Mét., Avril 1978.
14. Y. Meyzaud, Michaut and P. Parnière, Pub. Metals Society, n° 178, 1976,255-65.
15. S. Hanaï, N. Takemoto and Y. Mizuyama, Trans. ISIJ (11), 1971, 24-31.
16. R. Thibau, J. Masounave, R. Decelles and L. Piperni, I.C.S.M.A. 7 Montréal, Aug. 1985, vol. 3
17. R.P. Arthey and W.B. Hutchinson, Met. Trans.A, 12A, Oct. 1981, 1817.
18. Ch. Hénin and Ch. Brun, Rev. Mét. C.I.T., July 1981.
19. R. Ogawa, T. Fukutsuka and Y. Yagi, Trans. ISIJ (12), 1972, pp 291-7.
20. P.L. Antoniucci and JR. Ricci Bitti, ICOTOM 6 Int. Conf., Sept-Oct. 1981 Tokyo I.S.I.J.
21. F.J. Humphreys, Met. Sci., March-April 1979, Vol. 13, n° 3 and 4.
22. W.C. Leslie, R.L. Rickett, C.L. Dotson and C.S. Walton, Trans. ASM, Vol. 46, 1953.
23. M.J. Ashby, Phil. Mag., 1970, 21, 170, pp 399-424.
24. T. Ichiyama, M. Koizumi, I. Yoshida, K. Watanabe and S. Nishiumi, Trans. I.S.I.J., 1970, 10, n° 6, 429-41.
25. H. Hu, Met. Trans. A, Vol. 8A, Oct. 1977, 1567.
26. M. Hillert, Acta Met., Vol. 13, March 1965, 227.
27. Y. Meyzaud and P. Parnière, Mém. Sci. Rev. Mét., 71, n° 7 and 8, 1974.

28. D. Benoît-Bryckaert, Y. Meyzaud, P. Parnière and R. Tixier, IRSID report n° P235, May 1975.
29. T. Ichiyama, I. Yoshida, M. Ejima and D. Matsumura, Trans. I.S.I.J. report n° 2, 1975.
30. E. Furubayashi, H. Endo and H. Yoshida, Mat. Sci. Eng., 14, 1974, pp 123-30.
31. T. Chandra, I. Weiss and J. Jonas, Can. Met. Quat., vol. 20, n° 4, pp 421-8, 1981.
32. A.J. Ardell, Acta Met., vol. 20, Jan. 1972, p. 61.
33. E.I. Brown and E.J. Deardo, Thermomechanical processing of microalloyed austenite, Conf. Proc., Pittsburgh, 17-19 Aug. 1982, 319-41 Met. Soc., AIME
34 F. Vodopivec, J.I.S.I., Sept. 1973, pp. 664-5
35. J. Grewen, J. Huber and M. Hatherly, Met. Forum, Vol. 1, n° 3, Sept. 1978.
36. K. Matsudo, T. Shimomura and O. Nozoe, Texture of Crystalline Solids, 1978, Vol. 3, pp 53-72.

Pq, K^{-1}	10.74	9.58	9.82	9.28	9.72	9.23
H_R, °C/hr	28	28	40	40	55	55
T_m, °C	610	697	691	728	707	737
t_H, hr	10.7	24.7	12.5	22.3	9.7	16.0

Table 1. Thermal parameter (Pq), hearing rate (H_R), maximum temperature reached (T_m) and holding time (t_H) caracterizing six annealing treatments.

Steel	01	02	03	04	05	06	07	08
T_c,°C	690	570	700	570	680	540	700	550
C, %	.09		.06		.08		.07	
Al,% *	.063		.059		.042		.038	
N, ppm	81		50		70		64	
Mn,% **	.28		.32		.19		.21	

* total Al
**corrected following: Mn - (55/32)S

Table 2. Composition and coiling temperatures of the samples.

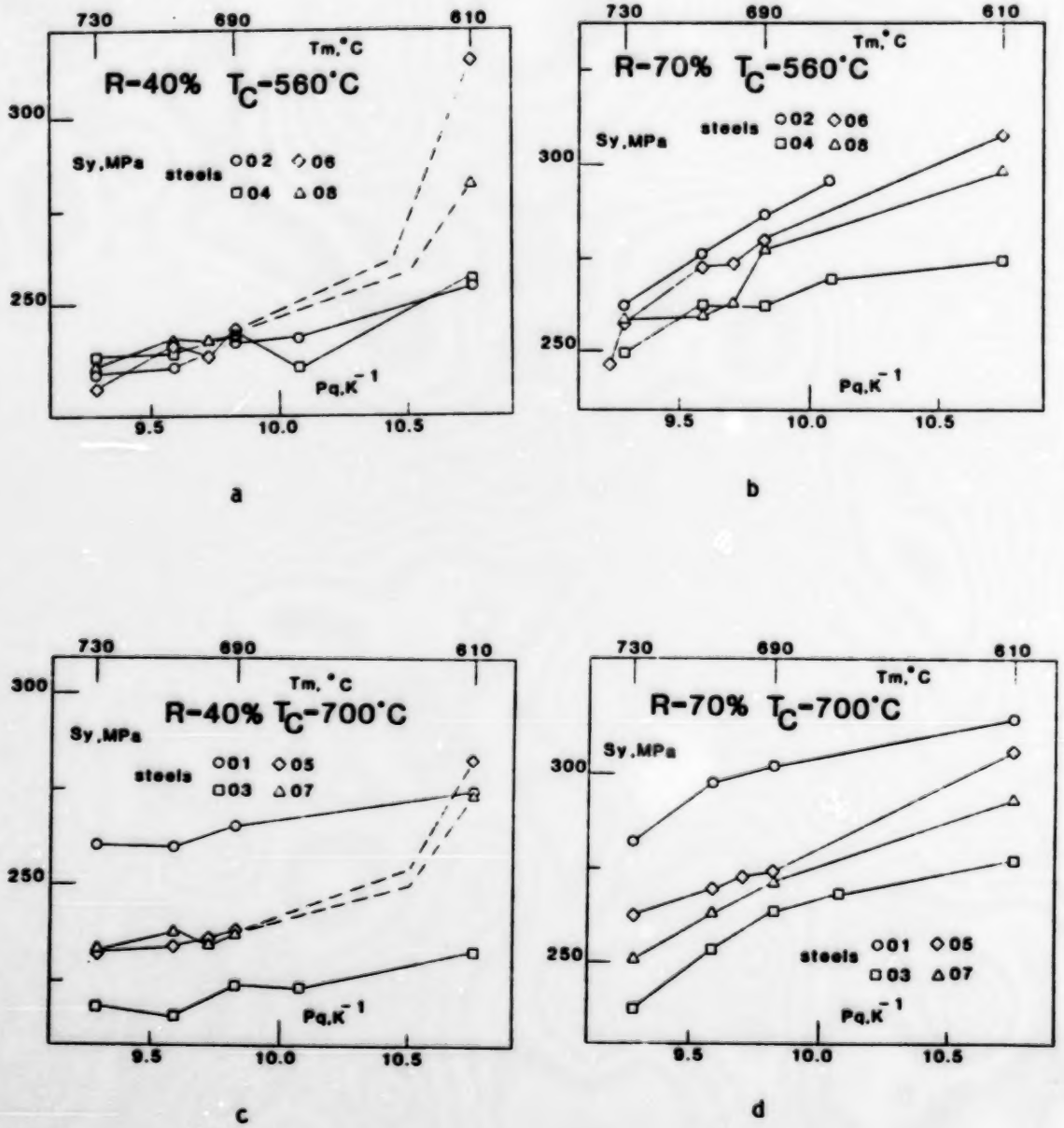

Fig. 1 Yied strength, Sy, vs thermal parameter, Pq, or maximum annealing temperature, Tm.

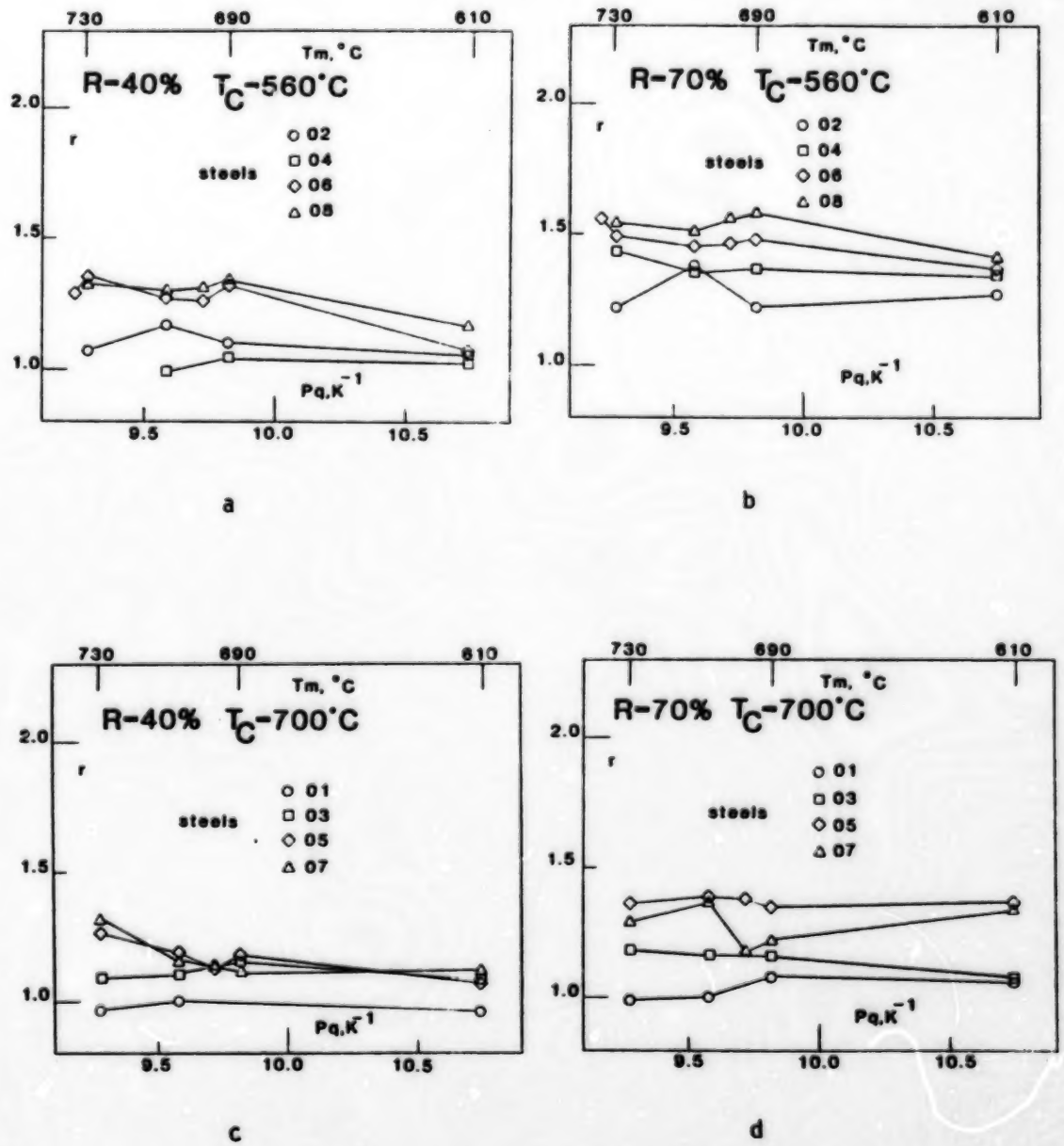

Fig. 2 Plastic anisotropy ratio, r, vs thermal paramater, Pq, or maximum annealing temperature, Tm.

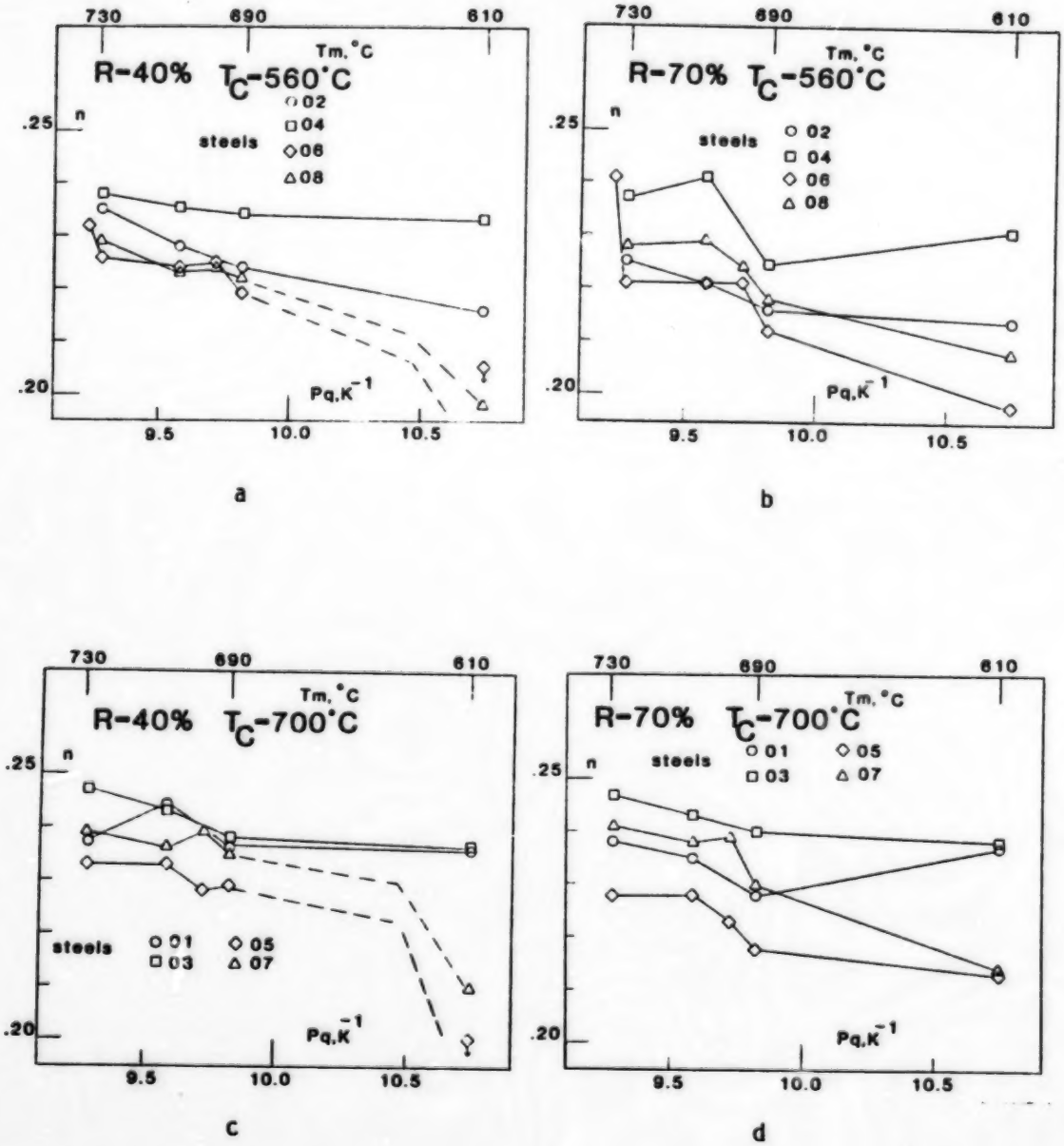

Fig. 3 Strain hardening rate, n, vs thermal paramater, Pq, or maximum annealing temperature, Tm.

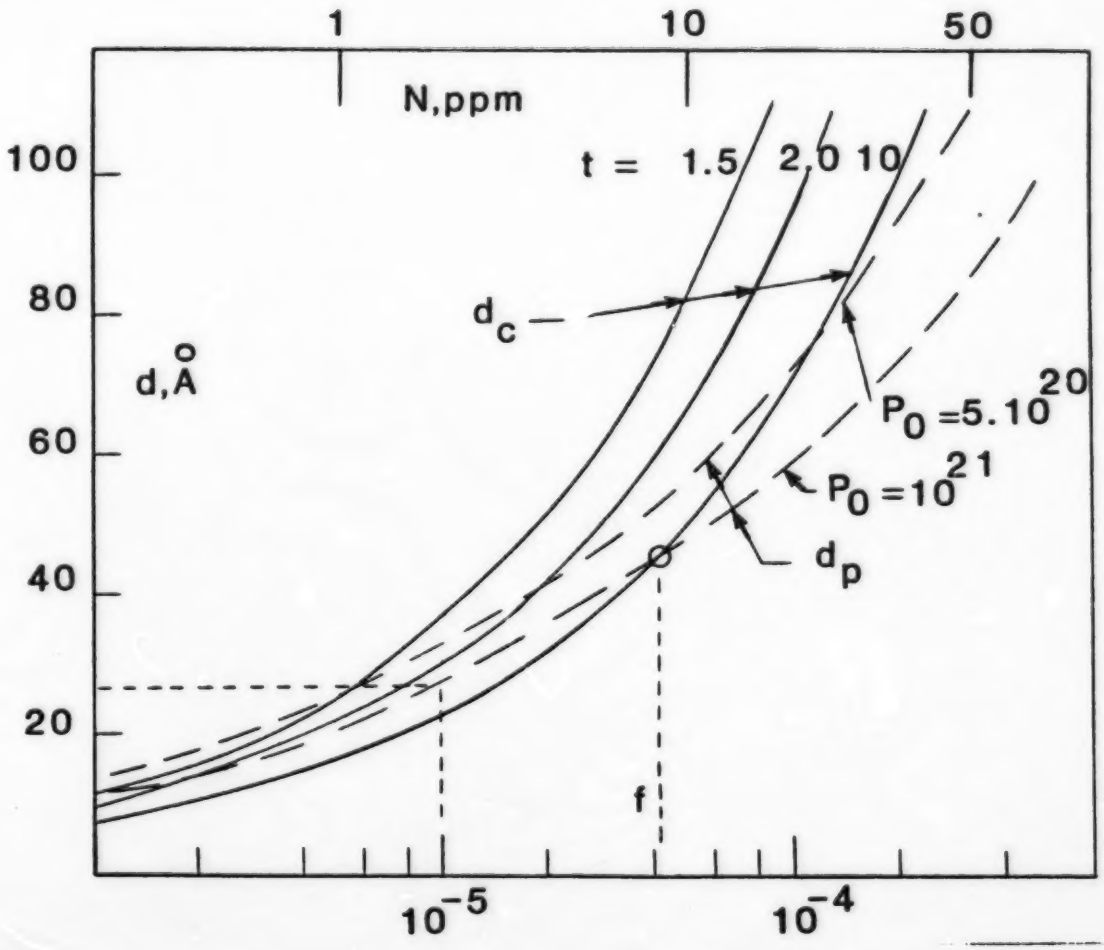

Fig. 4- AlN critical size, d_c, and AlN precipitate size, d_p vs AlN precipitated volume fraction, f, or precipitated nitrogen, N. Subgrain size is 1.0 mm, precipitation is on sub-boundaries and the number of precipitates on sub-boundaries is P_0.